

Correlation of Peak Wind Loads at Batten-Truss Connections

Korah Parackal, John Ginger and David Henderson

Cyclone Testing Station, College of Science Technology and Engineering,
James Cook University, Townsville, Queensland 4811, Australia

Abstract

Wind loads on roofs fluctuate significantly, both across their surfaces and in time. A 1/50 scale wind tunnel study was conducted to determine the correlations of these load fluctuations on batten to truss connections. This study found that load histories between neighbouring connections are correlated and are sensitive to wind direction. Critical wind directions that cause the highest uplift loads are not necessarily those that experience the highest correlations amongst neighbouring connections. Additionally, for different wind directions loads at connections to the left, right or diagonally across from the critical connections are more correlated, suggesting that the path that a progressive failure takes is dependent on wind direction and the location on the roof where it initiates.¹

Introduction

Damage to low-rise residential structures due to severe wind events remains a significant cause of economic loss to communities. Understanding the nature of loading and the response of connections to these loads is essential to be able to assess and reduce the vulnerability of houses to wind loading.

Due to aerodynamic effects, the usually sloping roofs of houses experience high negative pressures. In the case of light framed construction, these uplift loads can overcome the self-weight of the roof structure for wind loads above 35km/h (Reardon 1979). Recent damage surveys have shown that the failure of batten to truss/rafter connections are one of the more likely causes of roof damage from high wind events. These failures are especially the case when older structures are renovated and have new roof cladding placed on existing battens or have their cladding converted from tiles to metal sheeting (Parackal, Mason et al. 2015).

Wind loads on roof surfaces are highly fluctuating spatially as well as through time. These fluctuations can result in peak loads occurring at different batten to rafter connections and at different times. If certain connections weaken or begin to fail, load is transferred to adjacent connections rapidly. The time for load transfer within a structure being dependent on the speed of propagation of shear and bending waves that are related to the stiffness of the material.

Whether neighbouring connections also experience high loads at the same time determines whether they will be overloaded, potentially causing a progressive failure to initiate. Determining how these high loads across the roof surface are correlated is necessary to identify when and where cascading failures begin and which wind directions are critical.

Wind loading on low-rise buildings has been studied extensively. Holmes (1982), Ahmad and Kumar (2002) and Gavanski, Kordi et al. (2013), amongst others, have examined the pressure distributions across roof surfaces to determine the effects of roof pitch, upstream terrain, and wind direction. However, studies on the response of batten to rafter connections under fluctuating time history loads, the timing and correlation of high uplift loads experienced by these connections and the implications to progressive or cascading failures are limited.

Saathoff and Melbourne (1989) examined the formation and correlation of high negative pressures on the leading edge of rectangular bluff bodies for flow perpendicular to the edge of the body. Ginger and Letchford (1993) examined the correlation of wind pressure on a flat-roofed rectangular shaped building for two flow separation mechanisms: 2D flow separation when the wind is perpendicular to a leading edge and the 3D conical vortex formed for cornering wind directions. These studies found that pressures were correlated within these flow separation areas. However, it is unclear what kind of behaviour will be experienced for a typical sloped roof house.

Boughton, Falck et al. (2014) presents a reliability study of batten to truss connections for a contemporary Australian house. Fragility curves for various connection fasteners are developed for different roof areas (corner, edge and general). This study analysed the probabilities of 'first failure' of connections but did not examine what may be occurring to neighbouring connections at the time of failure.

The present study examines the timing and correlation of peak wind loads on batten to rafter connections on a typical gable roof house. Based on wind tunnel data, the nature and distribution of peak pressures for various wind directions is presented and discussed. For the critical wind direction, a more detailed analysis using the cross-correlation between time histories has been performed to show the timing of peak loads for neighbouring connections.

Wind Tunnel Tests

A 1/50 scale wind tunnel study was conducted to determine simultaneous loads at batten to truss connections for multiple wind directions. Tests were carried out in the 2.0m high × 2.5m wide × 22m long boundary layer wind tunnel at the Cyclone Testing Station, James Cook University.

The flow simulated in the wind tunnel was that of a suburban environment using an array of 50mm tall blocks on the upstream fetch of the wind tunnel. The model was placed on a turntable at the study area of the wind tunnel and pressure data at 10-degree

A similar paper is being submitted to the 24th Australasian Conference on the Mechanics of Structures and Materials (ACMSM24).

increments recorded to determine the effects of various wind directions on the pressures on the roof surface. A Turbulent Flow Instruments (TFI) ‘Cobra Probe’ was used to measure the approach wind velocity and turbulence intensity at various heights (z) above the floor of the tunnel as shown in Figure 1.

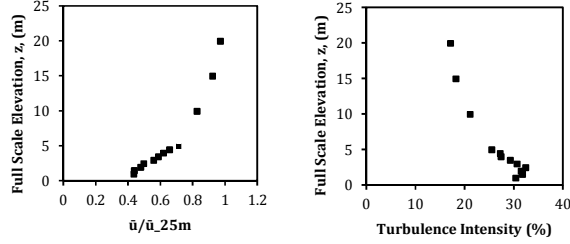


Figure 1 Boundary layer profiles simulated in the wind tunnel

A 1/50 scale model of a rectangular plan, gable roof house, shown in Figure 2, was used for this study. Based on survey data from Jayasinghe (2012), the model is of a 19.8m long by 10m wide house with a 22.5° roof pitch. Trusses and battens are spaced at 900mm and 877mm respectively supporting metal sheet cladding. As shown in Figure 3, trusses and battens are labelled as T1, T2...Tn and B1, B2...Bn, respectively. Batten to truss connections that were studied are labelled based on the Batten-Truss intersection T1-B3, T3-B4, etc. within the study area.

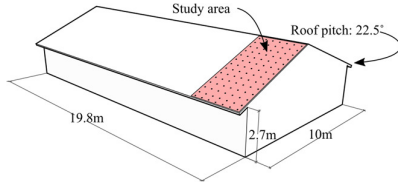


Figure 2 Study area of the wind tunnel model with full-scale dimensions

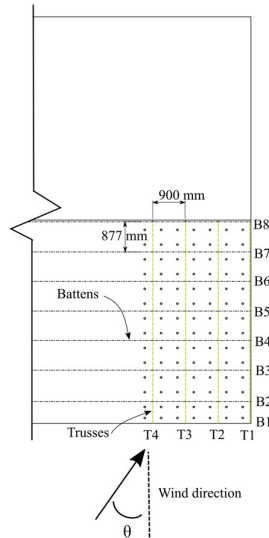


Figure 3 Tap layout and truss and batten locations in study area

Ninety-seven pressure taps were installed on a study area of the roof to capture the spatial and temporally varying pressures near the gable end section of the house. Pressure taps were arranged in a 450x439mm (full scale) grid pattern such that the 900x877mm tributary area of each batten to truss connection would include four pressure taps.

Pressure taps were connected to TFI pressure transducers and data acquisition system using a tuned tubing system. Data was low-pass filtered at 500 Hz and sampled at 1000Hz. Time history data for 24 runs of 30 seconds model scale (10 minutes full scale) were recorded for each wind direction.

The velocity in the wind tunnel was set at nominally 11m/s at z = 500mm height for a velocity ratio (Ur) of 2.5, this corresponds to 100km/h in full scale. For a Length scale (Lr) of 1/50, this corresponds to a time scale of 1/20. Thus, each 1/500 second time step recorded at model scale represents 0.04 seconds in full-scale time.

Pressures measured were represented as pressure coefficients C_p referenced to mid roof height of the wind tunnel model. The minimum, mean and standard deviation values were also recorded for each 30 second run and are given by:

$$\bar{C}_p = \frac{\bar{p} - p_0}{\frac{1}{2}\rho U_h^2} \quad \overline{C_p} = \frac{\bar{p} - p_0}{\frac{1}{2}\rho U_h^2} \quad C_{\sigma_p} = \frac{\sigma_p}{\frac{1}{2}\rho U_h^2}$$

Where,

- $\bar{p}, \sigma_p, \check{p}$ are the mean, standard deviation and minimum external pressures on the wind tunnel model
- p_0 is the reference free stream static pressure within the wind tunnel
- \overline{U}_h is the mean wind speed at mid-roof height (h) of the wind tunnel model
- ρ is the density of air

As described by Jayasinghe (2012), loads on batten-truss connections could be determined by taking the average pressure of taps within the tributary area of the batten to truss connection. For most connections this was four pressure taps, for connections on the roof edges, two taps, and one tap for corner connections. Loads at connections are presented in C_p form in this paper.

Correlation coefficients of load time histories at connections were determined to assess the timing of fluctuating loads from connection to connection. The correlation coefficient as a function of lag time (τ) of one signal relative to the other, or cross-correlation is defined as:

$$r_{ij} = \frac{1}{T * \sigma_{p_i} * \sigma_{p_j}} \int_0^T p'_i(t) * p'_j(t + \tau) dt \quad (1)$$

Where,

- p'_i and p'_j are the fluctuating components of the pressure at locations i and j.
- σ_p is the standard deviation of fluctuating load
- And T is the time over which the signal is analysed.

Results and Discussion

Pressure distributions and loads across the roof surface vary with wind direction. Plots of the average mean, minimum and standard deviation of batten-truss connection pressures C_p of the 24 ten-minute runs are shown in Figure 4. The highest negative pressures occur for wind directions 180° to 320°, the maximum load for all wind directions occurs at the connection at the ridgeline at the gable end for wind direction 210°

Correlation of Loads Amongst Neighbouring Connections

Connections at roof corners and at the apex of the gable end experience the highest peak loads for cornering winds. These loads are characterised by ‘peak events’ of load more than two standard deviations from the mean lasting about 0.5 to 2.0 seconds for a mean wind speed of 100 km/h at full scale. Figure 5 shows a 1-

minute (full scale) time history traces for a 3 × 3 grid of connections near the gable end of the ridgeline. Pressures are highly fluctuating and it can be seen that a peak event occurs for several of these connections around the same time.

The cross-correlation of the pressures within the roof area experiencing high loads was examined in detail to determine in what order the connections receive their highest loads. This analysis was performed for the same 3 × 3 grid of connections for the critical wind direction 210°. The cross-correlation of pressures on the selected connections to that of connection T1-B8 is shown in Figure 6 for lag time ± 0.4 seconds full scale.

Loads at connections T1-B7 and T2-B6, diagonally down from connection T1-B8, are the most correlated to the critical connection. An increase in correlation for lag times less than - 0.1 seconds indicate that pressure fluctuations move diagonally down the roof. Of note is that connection T2-B8, immediate neighbour to the left the critical connection is less correlated than several connections lower down the roof. As load will be redistributed along batten rows upon failure, it is possible that although wind direction 210° causes the maximum load at a connection, there may be other directions where loads are more correlated along batten rows and more conducive to progressive failures.

The cross-correlation analysis was repeated for wind direction 200°. The results presented in Figure 7 show that the correlation of pressures amongst neighbouring connections has a different pattern despite the small change in wind direction. The correlation of pressures to that of connection T1-B8 is noticeably higher than for the critical wind direction 210°. This indicates that wind directions that cause the highest uplift loads are not necessarily those that have the most correlated loads amongst neighbouring connections.

	0°	40°	90°	140°	180°	220°	270°	320°	
Min C _p	0.88 0.78 0.74 0.76 0.87 0.80 0.78 0.76 0.86 0.84 0.82 0.80 0.85 0.83 0.81 0.79 0.84 0.82 0.80 0.78 0.83 0.81 0.79 0.77 0.82 0.80 0.78 0.76 0.81 0.79 0.77 0.75 0.80 0.78 0.76 0.74	0.85 0.75 0.71 0.67 0.84 0.74 0.70 0.66 0.83 0.73 0.69 0.65 0.82 0.72 0.68 0.64 0.81 0.71 0.67 0.63 0.80 0.70 0.66 0.62 0.79 0.69 0.65 0.61 0.78 0.68 0.64 0.60 0.77 0.67 0.63 0.59	0.82 0.72 0.68 0.64 0.81 0.71 0.67 0.63 0.80 0.70 0.66 0.62 0.79 0.69 0.65 0.61 0.78 0.68 0.64 0.60 0.77 0.67 0.63 0.59 0.76 0.66 0.62 0.58 0.75 0.65 0.61 0.57 0.74 0.64 0.60 0.56	0.80 0.70 0.66 0.62 0.79 0.69 0.65 0.61 0.78 0.68 0.64 0.60 0.77 0.67 0.63 0.59 0.76 0.66 0.62 0.58 0.75 0.65 0.61 0.57 0.74 0.64 0.60 0.56 0.73 0.63 0.59 0.55 0.72 0.62 0.58 0.54	0.78 0.68 0.64 0.60 0.77 0.67 0.63 0.59 0.76 0.66 0.62 0.58 0.75 0.65 0.61 0.57 0.74 0.64 0.60 0.56 0.73 0.63 0.59 0.55 0.72 0.62 0.58 0.54 0.71 0.61 0.57 0.53 0.70 0.60 0.56 0.52	0.76 0.66 0.62 0.58 0.75 0.65 0.61 0.57 0.74 0.64 0.60 0.56 0.73 0.63 0.59 0.55 0.72 0.62 0.58 0.54 0.71 0.61 0.57 0.53 0.70 0.60 0.56 0.52 0.69 0.59 0.55 0.51 0.68 0.58 0.54 0.50	0.74 0.64 0.60 0.56 0.73 0.63 0.59 0.55 0.72 0.62 0.58 0.54 0.71 0.61 0.57 0.53 0.70 0.60 0.56 0.52 0.69 0.59 0.55 0.51 0.68 0.58 0.54 0.50 0.67 0.57 0.53 0.49 0.66 0.56 0.52 0.48	0.72 0.62 0.58 0.54 0.71 0.61 0.57 0.53 0.70 0.60 0.56 0.52 0.69 0.59 0.55 0.51 0.68 0.58 0.54 0.50 0.67 0.57 0.53 0.49 0.66 0.56 0.52 0.48 0.65 0.55 0.51 0.47 0.64 0.54 0.50 0.46	
Mean C _p	0.84 0.82 0.81 0.83 0.83 0.81 0.80 0.82 0.82 0.80 0.79 0.81 0.81 0.79 0.78 0.80 0.80 0.78 0.77 0.79 0.79 0.77 0.76 0.78 0.78 0.76 0.75 0.77 0.77 0.75 0.74 0.76 0.76 0.74 0.73 0.75	0.83 0.81 0.80 0.82 0.82 0.80 0.79 0.81 0.81 0.79 0.78 0.80 0.80 0.78 0.77 0.79 0.79 0.77 0.76 0.78 0.78 0.76 0.75 0.77 0.77 0.75 0.74 0.76 0.76 0.74 0.73 0.75 0.75 0.73 0.72 0.74	0.82 0.80 0.79 0.81 0.81 0.79 0.78 0.80 0.80 0.78 0.77 0.79 0.79 0.77 0.76 0.78 0.78 0.76 0.75 0.77 0.77 0.75 0.74 0.76 0.76 0.74 0.73 0.75 0.75 0.73 0.72 0.74 0.74 0.72 0.71 0.73	0.81 0.79 0.78 0.80 0.80 0.78 0.77 0.79 0.79 0.77 0.76 0.78 0.78 0.76 0.75 0.77 0.77 0.75 0.74 0.76 0.76 0.74 0.73 0.75 0.75 0.73 0.72 0.74 0.74 0.72 0.71 0.73 0.73 0.71 0.70 0.72	0.80 0.78 0.77 0.79 0.79 0.77 0.76 0.78 0.78 0.76 0.75 0.77 0.77 0.75 0.74 0.76 0.76 0.74 0.73 0.75 0.75 0.73 0.72 0.74 0.74 0.72 0.71 0.73 0.73 0.71 0.70 0.72 0.72 0.70 0.69 0.71	0.79 0.77 0.76 0.78 0.78 0.76 0.75 0.77 0.77 0.75 0.74 0.76 0.76 0.74 0.73 0.75 0.75 0.73 0.72 0.74 0.74 0.72 0.71 0.73 0.73 0.71 0.70 0.72 0.72 0.70 0.69 0.71 0.71 0.69 0.68 0.70	0.78 0.76 0.75 0.77 0.77 0.75 0.74 0.76 0.76 0.74 0.73 0.75 0.75 0.73 0.72 0.74 0.74 0.72 0.71 0.73 0.73 0.71 0.70 0.72 0.72 0.70 0.69 0.71 0.71 0.69 0.68 0.70 0.70 0.68 0.67 0.69	0.77 0.75 0.74 0.76 0.76 0.74 0.73 0.75 0.75 0.73 0.72 0.74 0.74 0.72 0.71 0.73 0.73 0.71 0.70 0.72 0.72 0.70 0.69 0.71 0.71 0.69 0.68 0.70 0.70 0.68 0.67 0.69 0.69 0.67 0.66 0.68	0.76 0.74 0.73 0.75 0.75 0.73 0.72 0.74 0.74 0.72 0.71 0.73 0.73 0.71 0.70 0.72 0.72 0.70 0.69 0.71 0.71 0.69 0.68 0.70 0.70 0.68 0.67 0.69 0.69 0.67 0.66 0.68 0.68 0.66 0.65 0.67
StdDev C _p	0.30 0.28 0.27 0.29 0.29 0.27 0.26 0.28 0.28 0.26 0.25 0.27 0.27 0.25 0.24 0.26 0.26 0.24 0.23 0.25 0.25 0.23 0.22 0.24 0.24 0.22 0.21 0.23 0.23 0.21 0.20 0.22 0.22 0.20 0.19 0.21	0.29 0.27 0.26 0.28 0.28 0.26 0.25 0.27 0.27 0.25 0.24 0.26 0.26 0.24 0.23 0.25 0.25 0.23 0.22 0.24 0.24 0.22 0.21 0.23 0.23 0.21 0.20 0.22 0.22 0.20 0.19 0.21 0.21 0.19 0.18 0.20	0.28 0.26 0.25 0.27 0.27 0.25 0.24 0.26 0.26 0.24 0.23 0.25 0.25 0.23 0.22 0.24 0.24 0.22 0.21 0.23 0.23 0.21 0.20 0.22 0.22 0.20 0.19 0.21 0.21 0.19 0.18 0.20 0.20 0.18 0.17 0.19	0.27 0.25 0.24 0.26 0.26 0.24 0.23 0.25 0.25 0.23 0.22 0.24 0.24 0.22 0.21 0.23 0.23 0.21 0.20 0.22 0.22 0.20 0.19 0.21 0.21 0.19 0.18 0.20 0.20 0.18 0.17 0.19 0.19 0.17 0.16 0.18	0.26 0.24 0.23 0.25 0.25 0.23 0.22 0.24 0.24 0.22 0.21 0.23 0.23 0.21 0.20 0.22 0.22 0.20 0.19 0.21 0.21 0.19 0.18 0.20 0.20 0.18 0.17 0.19 0.19 0.17 0.16 0.18 0.18 0.16 0.15 0.17	0.25 0.23 0.22 0.24 0.24 0.22 0.21 0.23 0.23 0.21 0.20 0.22 0.22 0.20 0.19 0.21 0.21 0.19 0.18 0.20 0.20 0.18 0.17 0.19 0.19 0.17 0.16 0.18 0.18 0.16 0.15 0.17 0.17 0.15 0.14 0.16	0.24 0.22 0.21 0.23 0.23 0.21 0.20 0.22 0.22 0.20 0.19 0.21 0.21 0.19 0.18 0.20 0.20 0.18 0.17 0.19 0.19 0.17 0.16 0.18 0.18 0.16 0.15 0.17 0.17 0.15 0.14 0.16 0.16 0.14 0.13 0.15	0.23 0.21 0.20 0.22 0.22 0.20 0.19 0.21 0.21 0.19 0.18 0.20 0.20 0.18 0.17 0.19 0.19 0.17 0.16 0.18 0.18 0.16 0.15 0.17 0.17 0.15 0.14 0.16 0.16 0.14 0.13 0.15 0.15 0.13 0.12 0.14	0.22 0.20 0.19 0.21 0.21 0.19 0.18 0.20 0.20 0.18 0.17 0.19 0.19 0.17 0.16 0.18 0.18 0.16 0.15 0.17 0.17 0.15 0.14 0.16 0.16 0.14 0.13 0.15 0.15 0.13 0.12 0.14 0.14 0.12 0.11 0.13

Figure 4 Mean (top row) minimum (middle) and standard deviation (bottom) pressure coefficients for the 32 connections in the study area for various wind directions.

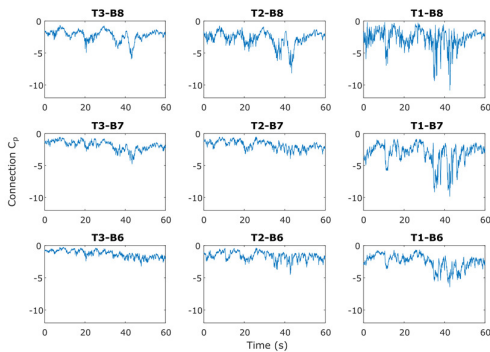


Figure 5 Time histories of C_p over a 9 × 9 grid of connections at the ridgeline.

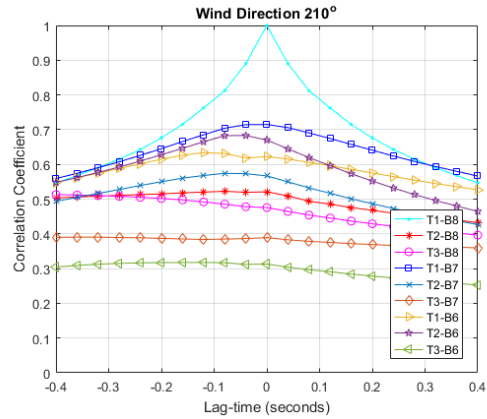


Figure 6 Correlation coefficient to connection T1-B8 vs. lag time for the critical wind direction 210°

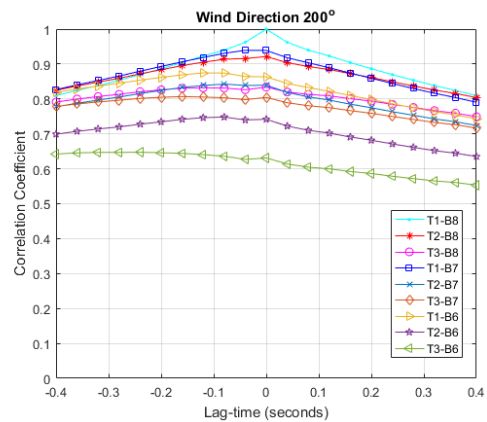


Figure 7 Correlation coefficient to connection T1-B8 vs. lag time for wind direction 200°

Distribution of Peak Load Areas

The peak loads experienced for various wind directions are due to different aerodynamic mechanisms. Thus, the timing, duration, location and correlation of the peak loads vary based on direction. Data were plotted on colour scale diagrams to show the loads on individual batten connections across the roof surface for each time step. When viewed as animation the pressure fluctuations due to the different flow separation regimes can be seen.

For the critical wind direction 210°, high uplift loads are experienced at the ridgeline and near the gable end of the roof. High negative pressures are experienced here consistently throughout time, shown in Figure 8. This is due to the inferred 3-dimensional flow separation region formed; indicated by the high standard deviations in this location, shown previously in Figure 4.

For the direction 180°, peak loads can occur over a large area of the leeward roof. Areas of negative pressures appear to roll down the leeward roof surface in bands repeatedly, as shown in Figure 9. Peak loads appear to be correlated along batten rows more than along rafters. Although the magnitude of peaks is significantly lower, the higher correlation along battens may make the roof more susceptible to progressive failures for this wind direction.

For the wind direction 270°, peak pressures occur in patches that move across the roof surface from the windward edge and along the crosswind length of the roof. The location from where the peak load areas originate at the leading edge moves up and down from the ridgeline to the roof corner repeatedly, shown in Figure 10. At this direction, peak loads can occur over a wide range of locations,

with the pressures correlated amongst the connections only in the peak load area. There appears to be an interaction with another flow separation regime at the ridgeline causing the peak load area to move up and down the roof surface.

As shown in Figure 11, for the cornering wind direction 300°, peak pressures are still experienced at the ridgeline that are correlated in a similar manner to direction 210°. Additionally, high uplift loads are also experienced about 1/3rd of the sloping distance from the roof corner. These peaks appear to be due to the formation of conical vortices that are an independent flow separation mechanism to that causing the peak pressures near the ridgeline. Pressures are more likely to be correlated diagonally upward from the leading edge than along batten rows.

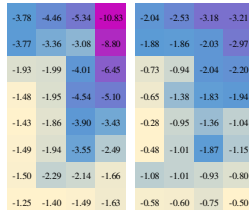


Figure 8 Load distribution (C_p) for wind direction 210°: during peak event (left) and during normal fluctuations (right).

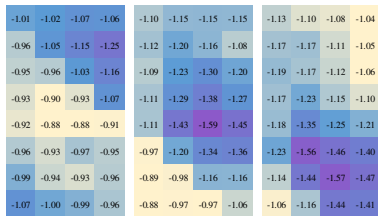


Figure 9 Successive time steps showing rolling peak load region on leeward roof for wind direction 180°



Figure 10 Successive time steps showing movement of peak load regions for wind direction 270°

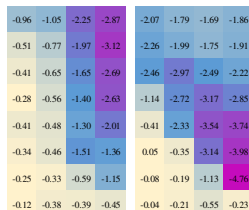


Figure 11 Peak load region at ridgeline due to flow separation (left) and due to conical vortex (right) for wind direction 300°

Conclusions and Further Work

The cross-correlation of signals shows that load time histories are indeed correlated and that peak loads are possibly correlated for neighbouring batten truss connections for a 900mm x 877mm truss and batten spacing. Lag times of peak correlation between connections give an indication of the direction that the peak load area is moving across the roof.

Depending on the wind direction, loads are correlated with connections either diagonally upward, downward or across from the critical connection. This has implications to progressive failures as wind directions that cause the greatest loads may not be the most conducive for the spread of failure across the roof. It was also found that wind directions causing the highest loads are not necessarily those that cause the highest correlations amongst neighbours.

For further work, cross-correlation analyses can be repeated for a range of wind directions. However, care must be taken to account for the movement of peak load areas across the roof surface. Conditionally sampled correlations of the signals during peak events may give a better indication of the correlation of peak pressures (values exceeding a certain threshold) during peak events. Finally, physical testing must be performed to quantify the connection response and load redistribution behaviour of batten-truss connections to assess the effect of correlated loads amongst neighbouring connections.

Acknowledgements: The authors are grateful for the support of the Commonwealth of Australia through the Bushfire and Natural Hazards Cooperative Research Centre.

References

Ahmad, S. and Kumar, K. (2002), "Wind pressures on low-rise hip roof buildings", *Wind and Structures*. 5(6), 493-514.

Boughton, G., Falck, D., Ginger, J.D., Henderson, D. and Satheeskumar, N. (2014). "Stochastic Models For Performance of Timber Roof Connections Under Wind Forces". *World Conference on Timber Engineering*, Quebec City, Canada, August 2014.

Gavanski, E., Kordi, B., Kopp, G.A. and Vickery, P.J. (2013), "Wind loads on roof sheathing of houses", *Journal of Wind Engineering and Industrial Aerodynamics*. 114(0), 106-121.

Ginger, J. and Letchford, C. (1993), "Characteristics of large pressures in regions of flow separation", *Journal of Wind Engineering and Industrial Aerodynamics*. 49(1), 301-310.

Holmes, J.D. (1982), *Wind pressures on houses with high pitched roofs*, Department of Civil and Systems Engineering, James Cook University of North Queensland

Jayasinghe, N.C. (2012), *The distribution of wind loads and vulnerability of metal clad roofing structures in contemporary Australian houses*, James Cook University, Townsville.

Parackal, K., Mason, M., Henderson, D., Stark, G., Ginger, J., Sommerville, L., Harper, B., Smith, D. and Humphreys, M. (2015), *Investigation of Damage: Brisbane, 27 November 2014 Severe Storm Event, Cyclone Testing Station, JCU, Report TR60*,

Reardon, G.F. (1979), *The Strength of Batten-to-rafter Joints: Test Results and Derivation of Design Loads*, Cyclone Testing Station, Department of Civil and Systems Engineering, James Cook University of North Queensland

Saathoff, P. and Melbourne, W. (1989), "The generation of peak pressures in separated/reattaching flows", *Journal of Wind Engineering and Industrial Aerodynamics*. 32(1), 121-134.